the FEBS Journal

Possible binding site for paclitaxel at microtubule pores

Matteo Magnani[1,*], Giorgio Maccari[1], José M. Andreu[2], J. F. Díaz[2] and Maurizio Botta[1]

1 Department of Pharmaceutical and Chemical Technology, Faculty of Pharmacy, University of Siena, Italy
2 Centro de Investigaciones Biologicas, Consejo Superior de Investigaciones Cientıficas, Madrid, Spain

Keywords
conformational analysis; hierarchical clustering; microtubule; paclitaxel

Correspondence
M. Botta, Department of Pharmaceutical and Chemical Technology, Faculty of Pharmacy, University of Siena, Via Aldo Moro 1, 53100 Siena, Italy
Fax: +39 05772 34333
Tel: +39 05772 34306
E-mail: botta@unisi.it
Website: http://www.unisi.it/ricerca/dip/dfct/

***Present address**
Siena Biotech SpA, Italy

(Received 20 January 2009, revised 18 February 2009, accepted 3 March 2009)

doi:10.1111/j.1742-4658.2009.06994.x

Taxanes and other microtubule-stabilizing agents comprise an important class of anticancer drugs. It is well known that taxanes act by binding to β-tubulin on the lumenal side of microtubules. However, experimental evidence obtained in recent years led to the hypothesis of an external site on the microtubule wall to which taxanes and other microtubule-stabilizing agents could bind before being internalized to their lumenal site. In the present study, different computational techniques were combined to explore the possible existence of an exposed and easily accessible binding site for microtubule-stabilizing agents on the outside of microtubules. The results obtained indicate that the conformational rearrangement of the H6–H7 hoop of β-tubulin can form a suitable pocket on the outer microtubule surface, and that paclitaxel can efficaciously interact with this newly-proposed binding site.

Microtubules are long, filamentous, tube-shaped protein polymers that are essential in all eukaryotic cells [1]. As key components of the cytoskeleton, they are crucial in the development and maintenance of cell shape, in the transport of vesicles, mitochondria and other components existing in cells, and in cell signaling and mitosis. Microtubules are produced by the assembly of α/β-tubulin heterodimers to form linear protofilaments, which laterally associate to form pseudohelical hollow tubes (the number of protofilaments is in the range 11–16) [2–5]. An essential feature for the activity of microtubules is their so-called 'dynamic instability'; they are highly-dynamic structures, comprising dimers that are continuously incorporated into the microtubule and released into solution in cells [6,7].

The role played by microtubules in mitosis makes them attractive targets for anticancer therapy [8], a perspective that has been explored using the so-called 'tubulin binding agents'. These compounds are able to disrupt microtubule dynamics and can act as either microtubule destabilizers (e.g. vinca alkaloids, colchicinoids or combretastatins) or microtubule stabilizers (e.g. taxanes or epothilones). Among the latter, the taxanes paclitaxel and docetaxel (Fig. 1) comprise well-known anticancer drugs that are currently being used in clinics for the treatment of several kinds of tumor, including ovarian, breast, head and neck, lung and prostate cancer [9,10]. These agents bind to tubulin in polymerized microtubules, resulting in the suppression of microtubule dynamics and the stabilization of the microtubules themselves, thus inducing mitotic arrest and, ultimately, cell death by apoptosis [11].

The taxane binding site on tubulin was experimentally determined approximately 10 years ago [1,12–14].

Abbreviations
MIF, molecular interaction field; MSA, microtubule-stabilizing agent.

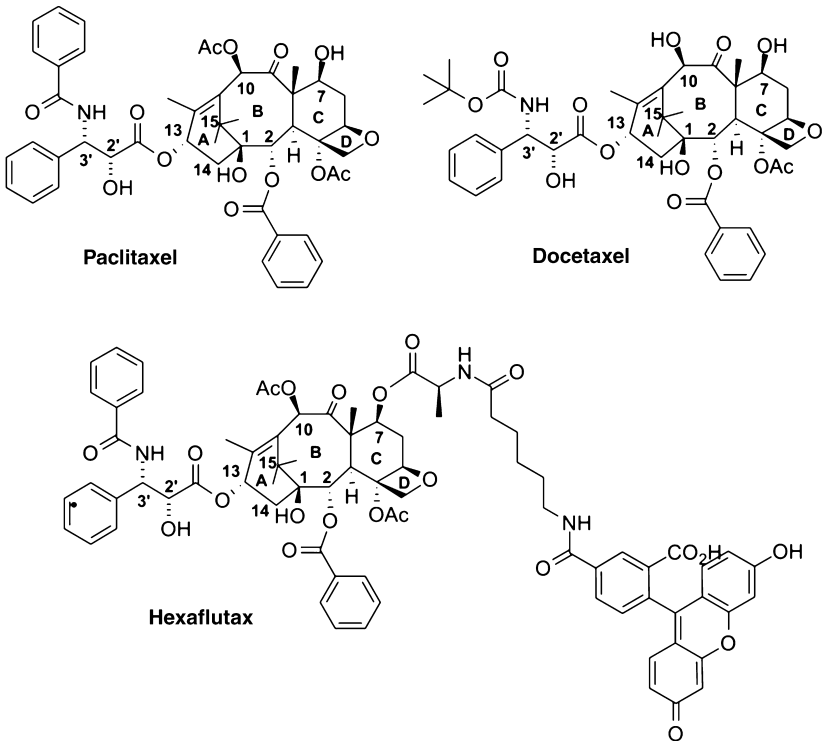

Fig. 1. Chemical structures of paclitaxel, docetaxel and hexaflutax.

The drugs were found to bind to the β-tubulin subunit on the microtubule inner surface; the accepted model held that taxanes and other microtubule-stabilizing agents (MSAs) would reach their binding pocket in the lumen of microtubules by diffusing through the fenestrations present on the microtubule wall.

However, in 2003, a study by Díaz *et al.* [15] revealed that the measured kinetics of paclitaxel binding to microtubules occurs too rapidly to be accounted for by diffusion through the microtubule pores; indeed, the size of pores is comparable with the dimension of the ligand, and they are therefore expected to slow down the diffusion process. These findings led the authors to hypothesize that paclitaxel could initially bind to an external (thus being easily accessible) site in microtubules, before its internalization in a subsequent step to reach the known inner site [15]. Such a mechanism would justify the observed rapid kinetics of binding and, at the same time, is in agreement with the final binding cleft in the microtubule interior. Because the stoichiometry of paclitaxel binding to α/β-tubulin is 1 : 1 [16], the external and the lumenal site must be mutually exclusive. In the same study, the loop between helices H6 and H7 of β-tubulin, as a result of its high flexibility and the presence of hydrophobic residues in which mutations are associated with paclitaxel resistance, was proposed to be involved in the preliminary binding of paclitaxel to the outer putative binding site, and to act as 'a lid that swings the ligand from the pore into the lumenal binding site' [17]. Such a loop surrounds pore type I (Fig. 2) and is also part of the lumenal site of MSAs [18–20].

Further studies demonstrated that a fluorescent taxoid, namely hexaflutax (Fig. 1), was able to bind to an external site on microtubules that is shared with paclitaxel, and that binding at this site is sufficient to induce microtubule assembly [21].

Because the kinetic rate of association of epothilone A to microtubules was shown to be almost identical to that of paclitaxel [22], it can be postulated that other MSAs binding at the paclitaxel internal pocket also could bind to the outer site before being internalized, thus making the existence of a binding site exposed on the microtubule wall an intriguing hypothesis. No less importantly, this putative site may also represent a second binding site for MSAs and therefore comprise a novel target for the rational design of antimitotic agents.

Consistent with the hypothesis of an external binding site for MSAs, Buey *et al.* [23] recently reported the natural compound cyclostreptin as a MSA acting with a novel mechanism of action. This agent was indeed found to covalently bind not only to Asn228, located in the lumenal paclitaxel site, but also to Thr220, residing within the previously mentioned H6–H7 loop [23]. Furthermore, microtubules incubated

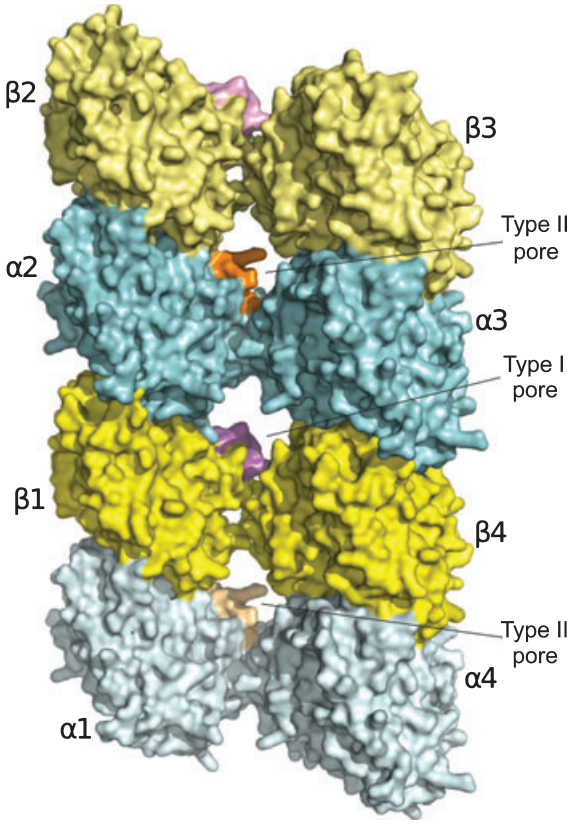

Fig. 2. Fragment of the microtubule wall structure, consisting of four α/β-tubulin heterodimers [24]. The microtubule is observed from the outside. Tubulin monomers surrounding pore type I are shown in bright colors. The H6–H7 loops of pore type I (β1-tubulin) and pore type II (α2-tubulin) are colored in magenta and orange, respectively.

with cyclostreptin lose the capacity to bind hexaflutax (J. F. Diaz & J. M. Andreu, unpublished data), which is a ligand that can only bind to the external surface of microtubules [21].

As a result, a novel model, which is gaining increasing acceptance, proposes that MSAs temporarily bind to an external low-affinity site on microtubules and then penetrate the pores to reach their final high-affinity site in the microtubule lumen [17,23].

In this context, we report the combination of different molecular modeling techniques aiming to gain insight, at the molecular level, on the possible existence of a binding site for MSAs at the outer microtubule surface. Based on the hypothesis proposed by Díaz *et al.* [15], our attention was initially focused on the region containing the H6–H7 loop of β-tubulin in pore type I (Fig. 2). Computational analysis showed that the rearrangement of the H6–H7 loop could result in the formation of a binding pocket on the external microtubule wall, which is sufficiently large to accommodate paclitaxel and other MSAs. Furthermore, on the basis of docking studies, two possible binding modes have been proposed for paclitaxel on the newly-identified outer site. Of note, when applied to pore type II, the same computational protocol was unable to identify a suitable binding pocket, thus suggesting the presence of an external binding site only on microtubules in pore type I.

Results and Discussion

The computational procedure set-up for the present study involved five sequential steps: (a) a preliminary analysis of the microtubule structure containing docetaxel bound to its lumenal site was performed, revealing the absence of a cavity suitable for ligand binding on the outer microtubule wall in proximity to the H6–H7 loop in pore type I. (b) Given the high flexibility of such a loop, a conformational study was carried out, aimed to explore its possible rearrangements and (c) the most representative structures resulting from conformational analysis were inspected for external binding pockets originating from the rearrangement of the H6–H7 loop. (d) Docking studies were then performed to assess the suitability of the detected cavities for paclitaxel binding, and to establish the potential binding mode of paclitaxel to the exterior location. Finally, (e) the structural features of the most interesting complexes derived from docking experiments were compared and analyzed. To better evaluate the results obtained for pore type I, steps (b) to (e) were also extended to pore type II, allowing for a comparison between the effects of the rearrangement of the H6–H7 loop in the two pores.

Analysis of the taxane-bound microtubule structure

For our computational study, we used a pseudo-atomic model of microtubules [24]. Such a model has been constructed by docking of an atomic structure of the α/β-tubulin heterodimer (Protein Databank code: 1TUB) [18], containing docetaxel bound to its inner site on the β subunit, into an experimental 20 Å resolution map of the microtubule [25]. In particular, our analysis was initially restricted to the four tubulin monomers bounding pore type I (Fig. 2), which comprised our main region of interest.

The tetramer under study, consisting of monomers belonging to four different α/β-tubulin heterodimers of two adjacent protofilaments and containing one bound docetaxel molecule, was first energy-minimized to remove some steric clashes present in the original model. The structure obtained was inspected using

POCKETPICKER [26], with the aim of identifying potential binding sites on the outer wall of the pore in proximity to the H6–H7 loop (Fig. 2, shown in magenta), the location suggested by Díaz *et al.* [15] for the external site. POCKETPICKER is a technique for the prediction and characterization of binding sites in proteins, based on the buriedness of points (among those placed at the edges of a grid containing the protein), which are located closely above the protein surface. The software clearly identified the lumenal binding site of MSAs, occupied by docetaxel. On the other hand, only one small pocket, mainly hydrophobic in character, was detected on the exterior of the tetramer in the region of interest, but its limited size made it unsuited for ligand binding. Such a pocket (Fig. 3) was located in the α subunit and was bounded by residues of helices H9 and H10 and the H8–H9 and S8–H10 loops; the secondary structure elements are labeled in accordance with a previous study [18].

The absence of putative binding pockets on the outer wall was not surprising because the experimental data suggested that binding to the external and lumenal site should be mutually exclusive. Accordingly, the external site should not exist on microtubules when a ligand is bound to the interior pocket.

However, the highly-flexible H6–H7 loop could adopt different conformations in the absence of bound ligands, thus forming (or concurring to form) a binding site on the outer microtubule surface. Consequently, we decided to perform a conformational analysis of the H6–H7 loop, aiming to evaluate whether the movement of the loop might be responsible for the formation of an external pocket potentially involved in the initial binding of paclitaxel (and, more generally, of other MSAs) to microtubules.

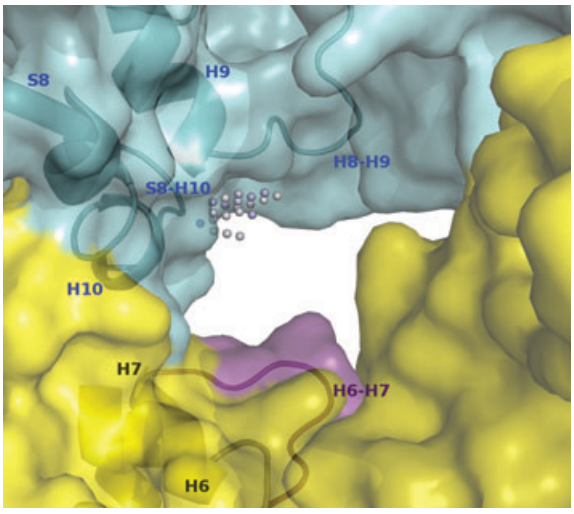

Fig. 3. Putative binding pocket detected by POCKETPICKER on the outer wall of microtubule when docetaxel is bound to the lumenal site. Similar to Fig. 2, α- and β-tubulin are colored in cyan and yellow, respectively, whereas residues of the H6–H7 loop are shown in magenta. According to the POCKETPICKER representation, the cavity is indicated by grid points with colors ranging from white to blue as the buriedness of the points increases. The microtubule wall is observed from the outside. No suitable cavity for binding was detected in close proximity to the H6–H7 loop.

Conformational analysis of the H6–H7 loop

As a first step, the original tetramer was energy minimized after removal of docetaxel. Subsequently, the H6–H7 loop (residues 217–223, residue numbers as in the 1TUB structure), was subjected to conformational analysis using the conformational search method for protein loops implemented in the MACROMODEL [27]. The conformational study provided almost 20 000 loop structures, which were subsequently subjected to cluster analysis to sample the wide conformational space through a restricted subset of structures. As a result, the whole set of conformations was partitioned into 174 clusters and, for each cluster, a representative conformation of the H6–H7 loop was selected and used for further analysis.

As shown in Fig. 4, the selected structures covered a broad region of space and, in most cases, this was characterized by conformations markedly different from that of the docetaxel-bound model.

Computational analysis suggested an oscillation movement of the H6–H7 loop with respect to its original conformation, directed toward either the inside or outside of the microtubule. Preliminary visual inspection of the selected structures revealed that, in some of them, especially those in which the H6–H7 loop folded toward the microtubule outside, the loop rearrangement gave rise to a cavity on the external tubulin surface. These findings were confirmed by subsequent POCKETPICKER analysis.

Search for putative binding sites on the outer wall of microtubules

Similar to the original tetramer, potential binding sites were sought using POCKETPICKER on the 174 tetramers characterized by the different conformations of their H6–H7 loops. Consistent with visual analysis, in several structures, POCKETPICKER identified variously sized pockets, located on the external surface of pore type I and bounded by the H6–H7 loop. More precisely, a pocket near the H6–H7 loop was revealed in 76 out of 174 tetramer structures. The presence of such pockets indicated that, by adopting a conformation different

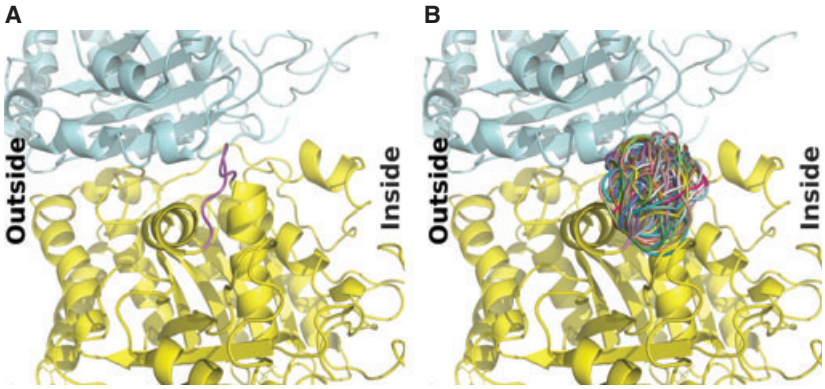

Fig. 4. (A) Structure of the H6–H7 loop (colored in magenta) in the original microtubule model. The loop is observed from the adjacent protofilament; the microtubule lumen is on the right. (B) The 174 structures of the H6–H7 loop are shown, as derived from the conformational search and subsequent cluster analysis.

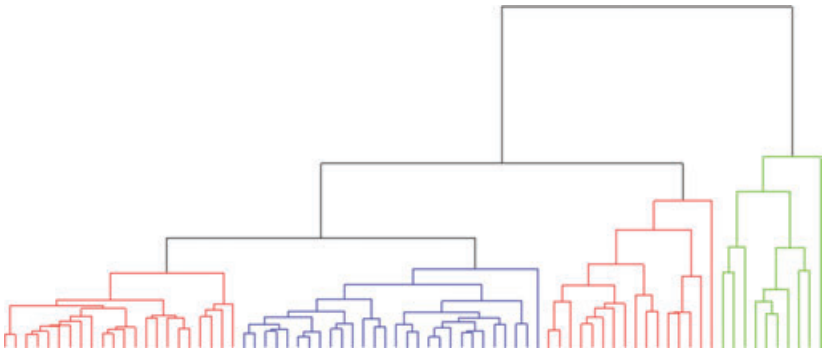

Fig. 5. Hierarchical tree corresponding to the cluster analysis performed on the 76 cavities detected by POCKETPICKER near the H6–H7 loop on the outer microtubule wall. The cavities are colored according to their size: small (red), medium (blue) and large (green). Small pockets are partitioned into two clusters as a result of differences in shape.

from that in which MSAs are bound to their lumenal site, the H6–H7 loop can play a fundamental role in forming a potential binding site on the outer surface of the microtubule.

Four hundred and twenty descriptors, codifying the shape and dimension of pockets, were computed by POCKETPICKER for all of the 76 cavities previously detected. A subsequent cluster analysis based on the POCKETPICKER descriptors led to the identification of four main subsets of cavities (Fig. 5). Essentially, they differed with respect to their dimensions, and were therefore classified into three classes: small, medium and large (containing 38, 28 and 10 pockets, respectively). Partitioning of small pockets in two different regions of the hierarchical tree was the result of differences in their shapes.

Only the large pockets, whose size was slightly smaller but comparable to that of the lumenal binding site, were retained for further investigation because they were deemed to be the most suitable for occupancy by large ligands such as paclitaxel and other MSAs. With respect to the position on the microtubule wall, all of the cavities were located at the interface between α- and β-tubulin, near the smaller pocket on the α subunit that also was found in the original tetramer structure. All of them were hydrophobic in character and very similar in terms of both shape and dimension. They were mainly bounded by helix H10 of α-tubulin and by helix H6 and the H6–H7 loop of β-tubulin. By adopting different conformations, in all of the pockets, the H6–H7 loop moved away from the lumenal binding site compared to the original structure. As an example, one of the pockets is shown in Fig. 6. Interestingly, the conformation of the H6–H7 loop that leads to the formation of a pocket on the outer wall of microtubules is similar to that found in the structure of tubulin bound to microtubule-destabilizing drugs (Protin Databank code: 1SA0) [28]. However, in the 1SA0 structure, the 'curved' conformation of tubulin makes the putative binding site inaccessible to ligands as a result of steric hindrance of helix H10 of α-tubulin (see Fig. S1).

The results provided by the computational analysis strongly support the newly-proposed model for binding of MSAs to microtubules, which claims the existence of a preliminary external binding site that is necessary for internalization to the final lumenal site. The existence of such a site is reinforced by the covalent binding of cyclostreptin to the external surface of microtubules, as revealed by the experimental data. Cross-linked microtubules (10 μM) were incubated with 15 μM cyclostreptin or dimethylsulfoxide overnight at 22 °C in glycerol assembly buffer and 0.1 mM GTP, and dialyzed for 5 h against the same solution. Hexaflutax (10 nM) was

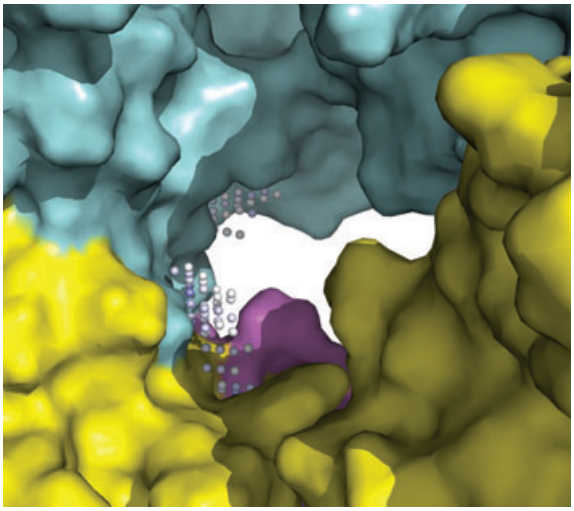

Fig. 6. POCKETPICKER representation of the binding pockets detected on the outer wall of microtubule in one of the structures derived from conformational analysis of the H6–H7 loop. Colors of grid points range from white to blue according to increasing buriedness; α- and β-tubulin subunits, as well as the H6–H7 loop, are colored as in Fig. 2. The microtubule wall is observed from the same side as shown in Fig. 3. The upper cavity was detected also in the docetaxel-bound microtubule, whereas the larger cavity at the α/β-tubulin interface was formed after rearrangement of the H6–H7 loop, which significantly concurs to bind it.

incubated in these preparations for 30 min at 25 °C, and the amount of bound hexaflutax was determined by a co-sedimentation assay, as described previously [21]. Although microtubules incubated with dimethylsulfoxide bind 7 μM hexaflutax, microtubules incubated with cyclostreptin lose their capacity to bind the external site ligand (J. F. Diaz & J. M. Andreu, unpublished data). Consistent with such an hypothesis, the present study showed that a putative binding site could form on the outer microtubule wall in proximity to pore type I, as a consequence of the oscillation of the H6–H7 loop.

Our models indicated that the external binding site is absent in microtubules when paclitaxel is bound to the inner site (Fig. 3) because the H6–H7 loop is involved in interactions with the drug. Conversely, in ligand-free microtubules, the H6–H7 loop can fold toward the outside of the wall, thus giving rise to the external binding site. These findings are in good agreement with mutually exclusive binding at the outer and lumenal site [15,21]; indeed, the two binding pockets could not be simultaneously occupied because the external one can only form (and thus ligands can bind to it) when the lumenal site is unoccupied and the H6–H7 loop is free to move. Finally, it should be noted that the proposed external binding site is formed by the α and β subunits of two distinct tubulin heterodimers; therefore, it can be observed only in assembled microtubules.

Suitability of the newly-identified pockets for paclitaxel binding

To continue our study, we aimed to assess whether some of the large pockets that were previously detected were suitable for binding of paclitaxel. The identification of plausible binding modes could significantly strengthen their role as putative external sites for paclitaxel and other MSAs, and comprise a preliminary validation of the location proposed for them on the microtubule wall. Accordingly, we performed docking studies to explore the possible binding modes of paclitaxel on the 10 large pockets identified in the previous step. Among the MSAs, we chose paclitaxel because the studies by Díaz *et al.* [15], which led to the proposal of the external binding site on microtubules, only focused on this well characterized ligand.

Docking experiments were carried out using AUTODOCK (http://autodock.scripps.edu), employing the Lamarckian genetic algorithm [29] to explore the orientation/conformational space of the ligand within the binding pocket. AUTODOCK analysis usually consists of several docking runs, each resulting in a predicted binding pose. The outputs of all runs are finally compared, and similar binding conformations are clustered together.

Preliminary docking experiments were carried out by applying different genetic algorithm parameter settings to simulate the binding mode of paclitaxel and docetaxel to the lumenal site, with experimental structures available as a reference [18,19]. The finally set-up protocol correctly reproduced the coordinates of both paclitaxel and docetaxel binding conformations, with the top scoring poses being the closest to the experimental binding modes and belonging to the most populated cluster. Remarkably, all of the known interactions between the protein and the ligands were identified [18,19,30]. Because the protocol was able to provide a reasonable prediction of the binding mode of paclitaxel and docetaxel, it was deemed reliable and thus applied in the subsequent docking analysis of paclitaxel on the external binding pockets.

AUTODOCK results were evaluated according to the predicted binding energy of both complexes and the cluster population. In addition, the location of the hydroxy group at C7 of paclitaxel was taken into account to select plausible binding modes. The last criterion takes into consideration the C7 position not appearing to be relevant for binding because modifica-

tions in this group do not alter the binding energy of paclitaxel analogs [31], and the incorporation of bulky groups [15,21,32] does not significantly alter their kinetics or binding affinity, thus suggesting that the C7 hydroxyl of paclitaxel should be exposed to the outer solvent when the ligand is bound to the external site on microtubules. Consequently, the proposed binding mode of paclitaxel to the putative exterior site was expected to be characterized by the positioning of the C7 hydroxy group toward the outside of the microtubule.

Significant docking results (i.e. complexes with low estimated binding energies and belonging to well-populated clusters) were obtained for nine out of the 10 pockets, whereas docking on the remaining cavity resulted in a huge number of clusters, which were scarcely populated and associated with high binding energies (thus giving no clear indication). The number of suitable complexes was further reduced to seven by discarding two binding modes in which the hydroxy group at C7 was directed toward the lumen of the microtubule.

Putative binding modes of paclitaxel to the outer surface of microtubules

The seven complexes derived from the docking studies were energy minimized and visually inspected. All of them were characterized by occupancy of both of the cavities detected by POCKETPICKER (Fig. 6), thus suggesting the presence of an external binding site mainly consisting of two hydrophobic pockets. Despite the different conformations adopted by the H6–H7 loop, only two distinct binding modes could be identified. The first one, afterwards referred to as 'binding mode I', was common to six of the seven complexes, and was therefore considered to be the most suitable. By contrast, the second binding mode, labeled as 'binding mode II', was found in only one complex.

In binding mode I (Fig. 7), the larger pocket at the α/β-tubulin interface was mainly occupied by the C2 benzoyl phenyl ring of paclitaxel, which established favorable hydrophobic interactions with Tyr β210, Phe β214, Thr β220 and/or Thr β221, Pro β222 and, to a lesser extent, with the alkyl chain of Lys α326. In some complexes, the carbonyl group of the benzoyl moiety was in hydrogen bond distance from the Lys α326 side chain. The baccatin core of the ligand was partially located in the same pocket, with the methyl groups at C15 interacting with the alkyl chain of Lys α326 and with Ala α330. The smaller cavity on the α subunit accommodated the C3′ phenyl ring, which was in van der Waals contact with Val α288, Val α323 and Val α324, as well as with the alkyl portion of the Asp α322 and Arg α373 side chains. Two hydrogen bonds were steadily observed between the carbonyl group of the benzamido moiety and the Arg α373 side chain, and between the C1′ carbonyl group and the backbone NH of either Val α288 and Ala α289. The C7 hydroxy group was directed toward the microtubule outside, thus making it possible to extend this binding model to fluorescent taxoids.

It is worth noting that one of the six complexes included in binding mode I was characterized by a different rearrangement of the side chain at C13; this resulted in a different location of the C3′ benzamido phenyl ring, in the loss of the previously described hydrogen bond involving the benzamido carbonyl group, and in the formation of a novel hydrogen bond between the benzamido NH and the Asp α327 side chain. However, in our opinion, these differences were not sufficient to consider the complex as being representative of a third binding mode.

In binding mode II (Fig. 8), the hydrophobic pocket formed by the rearrangement of the H6–H7 loop was occupied by the baccatin scaffold of paclitaxel, more precisely by its C and D rings, which established favorable contacts with Tyr β210, Phe β214, Thr β221 and Pro β222. The carbonyl group at C9 formed a hydrogen bond with the Lys α326 side chain, whereas one of the methyl groups at C15 had van der Waals contacts

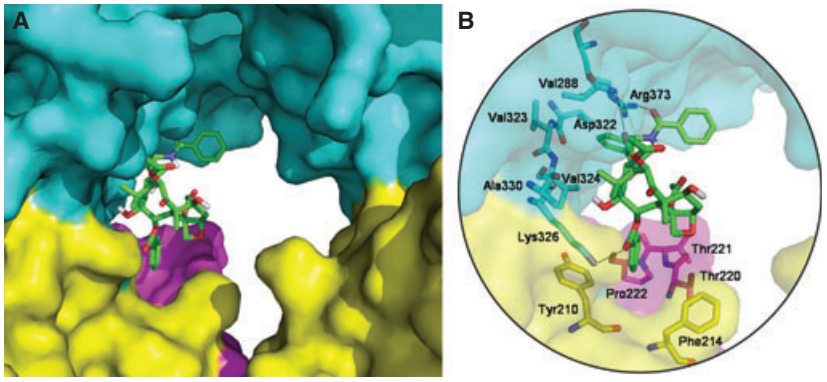

Fig. 7. (A) Representative structure of paclitaxel bound to the putative binding site for MSAs on the outer wall of the microtubule, according to binding mode I. Tubulin residues are colored as in Fig. 2, and paclitaxel is represented by green sticks. (B) Molecular detail of binding mode I. For clarity, only polar hydrogens of paclitaxel are shown.

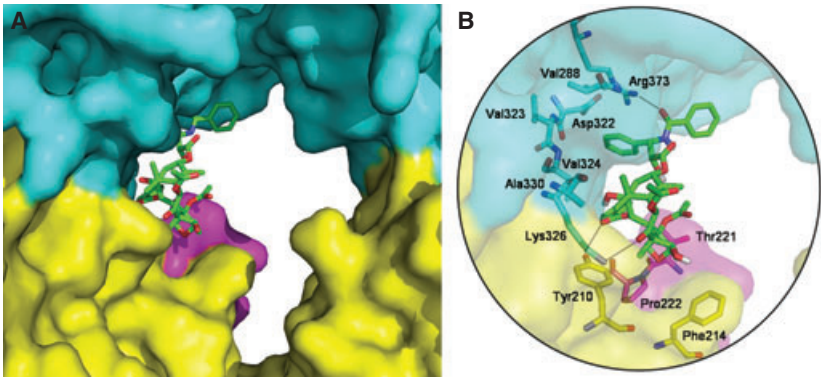

Fig. 8. (A) Paclitaxel bound to the putative binding site for MSAs on the outer wall of the microtubule, according to binding mode II. Tubulin residues are colored as in Fig. 2, and paclitaxel is represented by green sticks. (B) Molecular detail of binding mode II. For clarity, only polar hydrogens of paclitaxel are shown.

with the same chain and with Ala α330. The C2 benzoyl moiety was directed toward the lumen of the microtubule and was located in a groove bounded by Val α324 and Thr β221, with the carbonyl group being in hydrogen bond distance from the side chain of Tyr β210. The pose of the C13 side chain closely resembled that observed in binding mode I, with the C3′ phenyl ring embedded in the minor hydrophobic pocket of the binding site and the benzamido carbonyl group engaged in a hydrogen bond with the Arg α373 side chain. The C7 hydroxy group was still directed toward the microtubule outside.

The conformation of paclitaxel in the two binding modes closely resembled the T-taxol [33] conformation with respect to the orientation of side chains at C2, C4 and C10. On the other hand, significant differences were observed among the orientations of the C13 side chain in the three conformations (see Fig. S2).

Both poses proposed for the binding of paclitaxel to the external microtubule surface shared the occupancy of the two hydrophobic pockets detected by POCKETPICKER, and the energy values calculated for all of the minimized complexes were similar, thus not allowing discrimination between the two binding models. Although the number of complexes (six versus one) could indicate the binding mode I as being more probable, the available data are insufficient to discard binding mode II in favor of binding mode I. In this respect, additional experimental data would prove to be extremely valuable with respect to definitively selecting a putative binding mode and, more generally, validating the results obtained in the present study.

Analysis on pore type II

The 1 : 1 stoichiometry for paclitaxel binding to α/β-tubulin [15,21] indicates not only that binding to the external and lumenal sites is mutually exclusive, but also that paclitaxel cannot simultaneously bind to both pore I and pore II. Consistent with the hypothesis made by Díaz *et al.* [15], we initially focused on pore type I, and found it to be suitable for external binding of paclitaxel. However, if reliable, our computational procedure should also be able to discriminate between binding to pore I and pore II. For these reasons, we decided to perform the calculations described above on pore type II, which is bounded by the H6–H7 loop of α-tubulin (Fig. 2). The H6–H7 loops in α- and β-tubulin have the same length, although there are significant differences with respect to the nature of their residues because the β-tubulin H6–H7 loop has a prevalently hydrophobic character, whereas most of the residues comprising the H6–H7 loop of α-tubulin are polar or charged.

The tetramer under study in this case consisted of monomers belonging to two (instead of four) adjacent α/β-tubulin subunits. The conformational analysis of the H6–H7 loop resulted in approximately 11 000 different conformations, from which 128 representative structures were selected after clustering. In 82 of these structures, POCKETPICKER detected a cavity in proximity to the H6–H7 loop (i.e. similar to pore type I, a small cavity corresponding to that found in α-tubulin, and shown in Fig. 3, was constantly detected on the β-tubulin subunit as well), and the subsequent cluster analysis on the basis of POCKETPICKER descriptors led to the identification of ten pockets that were classified as large (Fig. 9), whose size and shape were comparable to those of the large pockets found in pore I.

Docking experiments were then carried out on the tetramers containing the 10 large pockets, although in no case was a suitable binding mode detected. Indeed, all of the docking runs resulted in poorly-populated clusters, with the best scoring poses often being singletons or those surrounded by a few neighbors.

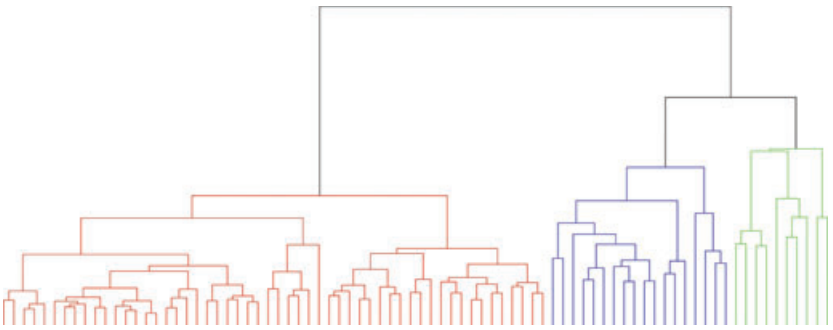

Fig. 9. Hierarchical tree for the 82 pockets found in pore type II. Pockets are color-coded as in Fig. 5.

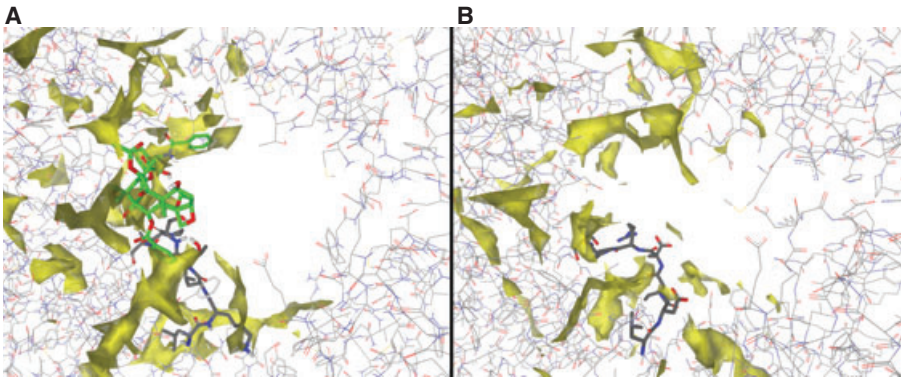

Fig. 10. MIFs calculated for the C3 probe on the putative outer binding site on (A) pore type I and (B) pore type II. Yellow maps indicate regions in which the interaction energy of the C3 probe with the protein is less than or equal to −0.8 kcal·mol^{-1}. Residues belonging to the H6–H7 loop are shown in stick representation. Paclitaxel is bound to pore type I according to binding mode I and is represented by green sticks. For both pore type I and II, MIFs relative to only one of the detected large pockets are displayed; however, similar results were obtained within each set of pockets.

To explain the differences of docking results between the pockets on pore type I and those on pore type II (despite their similarity in terms of size and shape), the two series of pockets were analyzed using GRID (version 22, Molecular Discovery Ltd., Pinner, UK) [34].

Molecular interaction fields (MIFs) were calculated in the putative binding sites for probes OH2, DRY and C3. The OH2 probe was used to describe hydrophilic interactions, whereas DRY and C3 probes were used to codify lipophilic interactions. The MIFs calculated for the OH2 probe were found to be substantially similar in the two sets of pockets. On the other hand, significant differences between pore types I and pore type II pockets were detected in MIFs derived from lipophilic probes, especially from the C3 probe. As shown in Fig. 10, the C3 probe appears to interact more favorably with the binding site on pore type I than with the binding site on pore type II. Similar, although less marked, differences were also observed for the DRY probe.

Remarkably, the regions that contributed most to differentiating between pore type I and pore type II pockets are those that are exploited by paclitaxel to interact with tubulin in both of the proposed binding modes on pore type I. Thus, despite the similarity in terms of volume and shape, the ligand appears to be unable to establish favorable hydrophobic interactions with pore type II, and this could account for the lack of significant docking results. Binding of paclitaxel in regions of favorable interactions for the C3 and DRY probes is in good agreement with the mainly hydrophobic nature of binding of the ligand [15]. Altogether, our analysis indicated that, in both pore types I and II, the rearrangement of the H6–H7 loop can form cavities on the outer surface of microtubules but, mainly as a result of differences in hydrophobic interactions, paclitaxel can efficaciously bind only to the pocket located in pore type I.

Conclusions

Different computational tools have been combined to obtain deeper insight into the presence of a putative binding site for taxanes and other MSAs on the exterior of microtubules, which should be occupied by the ligands before internalization into their lumenal

site. In addition to being necessary for penetrating the pores present on the microtubule surface, binding at this preliminary site would also be sufficient to achieve a stabilizing effect on microtubules. In the present study, the highly-flexible H6–H7 loop of tubulin was revealed to play a key role with respect to the existence and structure of a putative external binding pocket. Indeed, our analysis revealed that the conformational rearrangement of this loop could result in the formation of a cavity on the outer microtubule wall, and that such a pocket could only enable efficacious hydrophobic interactions with ligands in the case of pore type I. Two alternative binding modes have been proposed for paclitaxel into the modeled site. Taken together, the data obtained in the present study not only corroborate the recently proposed model of an external binding site on microtubules for MSAs, but also provide the molecular basis for the location of such a putative site at the interface between α- and β-tubulin subunits on pore type I.

Experimental procedures

Minimization of complexes

All of the energy minimizations (i.e. those of the original tetramers and those of complexes resulting from docking) were carried using AMBER 9 software [35]. Both the ff03 force field and the explicit solvent model TIP3P water were used. The structures were solvated with a truncated octahedron periodic water box, using a spacing distance of 10 Å around the molecule. The minimization process involved 1000 steepest-descent steps followed by 9000 conjugate gradient steps, until a convergence of 0.05 kcal·Å·mol^{-1} was reached.

Force field parameters for paclitaxel were generated with the antechamber and parmchk utilities, both implemented in the AMBER package, whereas those for GTP and GDP (located at the intra- and interdimer surface, respectively) were taken from the AMBER parameter database (http://pharmacy.man.ac.uk/amber).

Conformational analysis

The conformational search on the H6–H7 loop was performed using the MACROMODEL loop tool [36], using amber* as force field [37] and the implicit generalized Born/surface area water model to take into account solvent effects [38]. A substructure mask was applied on the system, leaving only the loop atoms free to move. Thirty thousand conformations were generated, and only those up to 200 kJ·mol^{-1} higher in energy than the global minimum were retained for further investigation.

Cluster analysis

For cluster analysis, we made use of bespoke software, which represents an application of the algorithm described by Kelley *et al*. [39]. All of the structures of the H6–H7 loop obtained from conformational analysis were initially clustered by the complete linkage method, on the basis of the rmsd values calculated taking into account all nonhydrogen atoms of the loop. Subsequently, an automated method was used to identify the optimal number of clusters in which the set of structures had to be partitioned to allow selection of the minimum number of representative structures, with the minimum being the loss of structural information (an example of application is provided in Hasel *et al*. [38]), resulting in a rmsd threshold value of 1.1 Å. Finally, for each cluster, the software provided a representative structure as output, which was the nearest to the mean coordinates of the structures belonging to the cluster itself.

Search for binding sites

The presence of putative binding sites on tubulin was evaluated using POCKETPICKER [26], a plug-in for PYMOL [40]. POCKETPICKER performs grid-based scanning on the protein using the buriedness of grid point as a parameter to define potential binding pockets. POCKETPICKER analysis results in groups of grid points describing the shape and accessibility of the detected pockets. Furthermore, for each pocket, a wide set of descriptors is computed that codify its shape and buriedness. Two parameters were modified with respect to the default values: (a) the grid spacing value (i.e. the mesh size of the grid), which was raised from 1.0 to 1.25 Å, and (b) the outer cut-off value (i.e. the maximal distance that grid points should have from the closest protein atom to be considered for pocket detection), which was raised from 4.5 to 6.5 Å. The descriptors characterizing all of the pockets originating from the rearrangement of the H6–H7 loop were used for cluster analysis of the pockets, which was performed using the same bespoke software described above.

Docking into the external pockets

All of the docking simulations were performed with AUTODOCK, version 4.0 (http://autodock.scripps.edu). A number of trials allowed identification of the best genetic algorithm parameters for reproducing the experimental binding modes of paclitaxel and docetaxel. As a result, the number of individuals within the population and the number of runs were set to 250 and 255, respectively. A maximum number of 5×10^6 energy evaluations and 2.7×10^5 generations was allowed. The mutation rate, the cross-over rate and the probability of local search were set to 0.02, 0.8 and 0.1, respectively. Notably, the use of the arithmetic cross-over

mode [41] allowed the software to markedly improve its performance with respect to correctly reproducing the experimental data (in particular, a significant increase in the number of correct binding modes for the final set of solutions was observed). The mutation step sizes were set to 1.0 Å (translation) and to 25.0° (torsional and quaternion). Finally, the 255 structures were clustered using an rmsd tolerance of 2.5 Å.

GRID calculations

Computation of MIFs over the putative binding sites was carried out using GRID, version 22. Box dimensions were defined to accommodate all the residues constituting and surrounding the binding sites, and the NPLA parameter (i.e. number of planes of grid points per angstrom) was set to 1. MIFs were computed for probes C3, DRY and OH2.

References

1 Downing KH & Nogales E (1998) Tubulin and microtubule structure. *Curr Opin Cell Biol* **10**, 16–22.

2 Andreu JM, Bordas J, Díaz JF, García de Ancos J, Gil R, Medrano FJ, Nogales E, Pantos E & Towns-Andrews E (1992) Low resolution structure of microtubules in solution. Synchrotron X-ray scattering and electron microscopy of taxol-induced microtubules assembled from purified tubulin in comparison with glycerol and MAP-induced microtubules. *J Mol Biol* **226**, 169–184.

3 Mandelkow EM, Schulteiss R, Rapp R, Müller M & Mandelkow E (1986) On the surface lattice of microtubules: helix starts protofilament number seam and handedness. *J Cell Biol* **102**, 1067–1073.

4 Wade RH, Chrétien D & Job D (1990) Characterization of microtubule protofilament numbers. How does the surface lattice accommodate? *J Mol Biol* **212**, 775–786.

5 Díaz JF, Valpuesta JM, Chacón P, Diakuni G & Andreu JM (1998) Changes in microtubule protofilament number induced by taxol binding to an easily accessible site. *J Biol Chem* **273**, 33803–33810.

6 Valiron O, Caudron N & Job D (2001) Microtubule dynamics. *Cell Mol Life Sci* **58**, 2069–2084.

7 Desai A & Mitchison TJ (1997) Microtubule polymerization dynamics. *Annu Rev Cell Dev Biol* **13**, 83–117.

8 Jordan MA & Wilson L (2004) Microtubules as a target for anticancer drugs. *Nat Rev Cancer* **4**, 253–265.

9 Slichenmyer WJ & Von Hoff DD (1991) Taxol: a new and effective anti-cancer drug. *Anticancer Drugs* **2**, 519–530.

10 Choy H (2001) Taxanes in combined modality therapy for solid tumors. *Crit Rev Oncol Hematol* **37**, 237–247.

11 Horwitz SB (1992) Mechanism of action of taxol. *Trends Pharmacol Sci* **13**, 134–136.

12 Rao S, Krauss NE, Heerding JM, Swindell CS, Ringel I, Orr GA & Horwitz SB (1994) Characterization of two taxol photoaffinity analogues bearing azide and benzophenone-related photoreactive substituents in the A-ring side chain. *J Biol Chem* **269**, 3132–3134.

13 Rao S, Orr GA, Chaudhary AG, Kingston DG & Horwitz SB (1995) Characterization of the taxol binding site on the microtubule. 2-m-Azidobenzoyl.taxol photolabels a peptide amino acids 217-231. of beta-tubulin. *J Biol Chem* **270**, 20235–20238.

14 Rao S, He L, Chatkravarty S, Ojima I, Orr GA & Horwitz SB (1999) Characterization of the taxol binding site on the microtubule. Identification of Arg282. in beta-tubulin as the site of photoincorporation of a 7-benzophenone analogue of taxol. *J Biol Chem* **274**, 37990–37994.

15 Díaz JF, Barasoain I & Andreu JM (2003) Fast kinetics of taxol binding to microtubules. *J Biol Chem* **278**, 8407–8419.

16 Díaz JF & Andreu JM (1993) Assembly of purified GDP-tubulin into microtubules induced by taxol and taxotere: reversibility, ligand stoichiometry, and competition. *Biochemistry* **32**, 2747–2755.

17 Snyder JP (2007) The microtubule-pore gatekeeper. *Nat Chem Biol* **3**, 81–82.

18 Nogales E, Downing KH & Wolf SG (1998) Structure of the α/β tubulin dimer by electron crystallography. *Nature* **391**, 199–203.

19 Löwe J, Li H, Downing KH & Nogales E (2001) Refined structure of αβ-tubulin at 3.5 Å resolution. *J Mol Biol* **313**, 1045–1057.

20 Nettles JH, Li H, Cornett B, Krahn JM, Snyder JP & Downing KH (2004) The binding mode of epothilone A on αβ-tubulin by electron crystallography. *Science* **305**, 866–869.

21 Díaz JF, Barasoain I, Souto AA, Amat-Guerri F & Andreu JM (2005) Macromolecular accessibility of fluorescent taxoids bound at a paclitaxel binding site in the microtubule surface. *J Biol Chem* **280**, 3928–3937.

22 Díaz JF & Buey RM (2007) Characterizing ligand-microtubule binding by competition methods. *Methods Mol Med* **137**, 245–260.

23 Buey RM, Calvo E, Barasoain I, Pineda O, Edler MC, Matesanz R, Cerezo G, Vanderwal CD, Day BW, Sorensen EJ *et al.* (2007) Cyclostreptin binds covalently to microtubule pores and lumenal taxoid binding sites. *Nat Chem Biol* **3**, 81–82.

24 Chacon P & Wriggers W (2002) Multi-resolution contour-based fitting of macromolecular structures. *J Mol Biol* **371**, 375–384.

25 Sosa H, Dias DP, Hoenger A, Whittaker M, Wilson-Kubalek E, Sablin E, Fletterick RJ, Vale RD & Milligan RA (1997) A model for the microtubule-Ncd motor protein complex obtained by cryo-electron microscopy and image analysis. *Cell* **90**, 217–224.

26 Weisel M, Proschak E & Schneider G (2007) PocketPicker: analysis of ligand binding-sites with shape descriptors. *Chem Cent J* **1**, 7.
27 Mohamadi F, Richards NGJ, Guida WC, Liskamp R, Lipton M, Caufield C, Chang G, Hendrickson T & Still WC (1990) MacroModel – an integrated software system for modeling organic and bioorganic molecules using molecular mechanics. *J Comput Chem* **11**, 440–467.
28 Ravelli RB, Gigant B, Curmi PA, Jourdain I, Lachkar S, Sobel A & Knossow M (2004) Insight into tubulin regulation from a complex with colchicine and a stathmin-like domain. *Nature* **428**, 192–202.
29 Morris GM, Goodsell DS, Halliday RS, Huey R, Hart WE, Belew RK & Olson AJ (1998) Automated docking using a Lamarckian genetic algorithm and an empirical binding free energy function. *J Comput Chem* **19**, 1639–1662.
30 Snyder JP, Nettles JH, Cornett B, Downing KH & Nogales E (2000) The binding conformation of taxol in β-tubulin: a model based on electron crystallographic density. *Proc Natl Acad Sci USA* **98**, 5312–5316.
31 Matesanz R, Barasoain I, Yang C, Wang L, Li X, de Ines C, Coderch C, Gago F, Barbero JJ, Andreu JM *et al.* (2008) Optimization of taxane binding to microtubules: binding affinity dissection and incremental construction of a high-affinity analog of paclitaxel. *J Chem Biol* **15**, 573–585.
32 Díaz JF, Strobe R, Engelborghs Y, Souto AA & Andreu JM (2000) Molecular recognition of taxol by microtubules. *J Biol Chem* **34**, 26265–26276.
33 Kingston DGI, Bane S & Snyder JP (2005) The taxol pharmacophore and the T-taxol bridging principle. *Cell Cycle* **4**, 279–289.
34 Reynolds CA, Wade RC & Goodford PJ (1989) Identifying targets for bioreductive agents: using GRID to predict selective binding regions of proteins. *J Mol Graph* **7**, 103–108.
35 Case DA, Darden TA, Cheatham TE, Simmerling CL, Wang J, Duke RE, Luo R, Merz KM, Pearlman DA, Crowley M *et al.* (2006) *AMBER9*. University of California, San Francisco, CA Available at: http://amber.ch.ic.ac.uk.
36 Mohamadi F, Richards NGJ, Guida WC, Liskamp R, Lipton M, Caufield C, Chang G, Hendrickson T & Still WC (1990) MacroModel – an integrated software system for modeling organic and bioorganic molecules using molecular mechanics. *J Comput Chem* **11**, 440–467.
37 Weiner SJ, Kollman PA, Case DA, Singh UC, Chio C, Alagona G, Profeta S & Weiner P (1984) A new force field for molecular mechanical simulation of nucleic acids and proteins. *J Am Chem Soc* **106**, 765–784.
38 Hasel W, Hendrickson TF & Still WC (1998) A rapid approximation to the solvent accessible surface areas of atoms. *Tetrahedron Comput Methodol* **1**, 103–116.
39 Kelley LA, Gardner SP & Sutcliffe MJ (1996) An automated approach for clustering an ensemble of NMR-derived protein structures into conformationally-related subfamilies. *Protein Eng* **9**, 1063–1065.
40 Delano WL (2002) *The PyMOL Molecular Graphics System*. DeLano Scientific, Palo Alto, CA. Available at: http://www.pymol.org.
41 Thomsen R (2003) Flexible ligand docking using evolutionary algorithms: investigating the effects of variation operators and local search hybrids. *BioSystems* **72**, 5773.

Supporting information

The following supplementary material is available:
Fig. S1. Comparison between the 'curved' conformation of tubulin bound to microtubule-destabilizing drugs (magenta; Protein Databank code: 1SA0) and the 'straight' conformation of tubulin, which accommodates the putative external site (cyan).
Fig. S2. Comparison between the alternative conformations of paclitaxel bound to the newly-proposed binding site on the outer surface of microtubules and the conformation of paclitaxel bound to the lumenal binding site of microtubules.

This supplementary material can be found in the online version of this article.

Please note: Wiley-Blackwell is not responsible for the content or functionality of any supplementary materials supplied by the authors. Any queries (other than missing material) should be directed to the corresponding author for the article.